Chapter 4
Research Microplastics—Hydraulic Size of Microplastic Particles of Regular Shape and Their Distribution Over the Depth of the Watercourse

N. R. Akhmedova and V. A. Naumov

Abstract Features of calculating the settling velocity of microplastic particles (MP) of regular shape and their distribution over the watercourse depth are considered in the article. The balance equation of forces acting on the MP particle is solved numerically to determine the settling rate. In this case, the previously obtained dependence of the hydrodynamic drag coefficient on the Reynolds number and the particle shape is used. The method for constructing a profile of the MP distribution over the depth of a steady flow depending on the shape, size, and density of particles, and the average velocity of the watercourse is proposed. This profile allows you to calculate the average vertical concentration by measuring the MP concentration near the surface of the watercourse.

Keywords Microplastic · Hydraulic size · Settling rate

4.1 Introduction

The problem of environmental pollution by small particles (less than 5 mm) from polymer materials has become very relevant in the twenty-first century. These particles are called microplastics (MP). Initially, most research was carried out on the distribution of MP in the World's Oceans (see Andrady 2011; Chubarenko and Stepanova 2017; Cózar et al. 2014; Erni-Cassola et al. 2019). Gradually, it became clear that it is equally important to study the sources and ways of MP migration along rivers.

The contribution of a large urban area to MP pollution of the Los Angeles and San Gabriel rivers was evaluated in (Moore et al. 2011). Samples were obtained using nets from the mass ejection sites of MP. The nets made it possible to select particles larger than 1 mm. The number of plastic objects and fragments for 72 h of observations exceeded 2 billion with a total weight of more than 30 thousand kg. Bottom sediments

N. R. Akhmedova (✉) · V. A. Naumov
Kaliningrad State Technical University, Sovetsky prospect 1, 236022 Kaliningrad, Russian Federation
e-mail: isfendi@mail.ru

A. G. Arkhipov (ed.), *Sustainable Fisheries and Aquaculture: Challenges and Prospects for the Blue Bioeconomy*, Environmental Science and Engineering, https://doi.org/10.1007/978-3-031-08284-9_4

over 320 km of the Saint Lawrence river were studied in (Castañeda et al. 2014). Plastic beads were found in all samples. The average bead size was 0.7 mm in areas receiving municipal or industrial runoff. The concentration at different sites varied from 52 to 13,832 units per square meter of the bottom.

The results of the study of MP pollution on the surface of the Rhine River are presented in the article (Mani et al. 2015). Measurements were made at 11 points over 820 km. MP concentrations were varied along and across the river. The beads were predominant among the detected particles (58.5%). The authors (Mani et al. 2015) explain this fact by the widespread use of such particles in the manufacture of products made of polymer materials, as cleaning granules, and in other industries. Fragments of MP (37.5%) and fibers (2.5%) are formed as a result of destruction or abrasion of larger plastic products. Polystyrene was the dominant polymer among MP (29.7%).

The composition of MP in the surface waters of the lower Yellow River near the mouth was studied in (Han et al. 2020). Fibers accounted for more than 93%. Almost 88% of the particles in the river's surface waters were less than 0.2 mm. Infrared spectrometric analysis showed the following MP materials: polyethylene, polypropylene and polystyrene. The average MP content in the dry and wet seasons was 930 and 497 units per liter, respectively.

The aquaculture was the main source of MP pollution in the mouth of the Qin River (China) (Zhang et al. 2020). Surface water and sediment samples were collected using plankton nets at 12 points along the urban section of the river. Fibers made up the majority in surface waters. Particles of 1–5 mm in size predominated in the bottom sediments. Particles from polyethylene and polypropylene made up about 70%.

The results of studying MP at three stratified depths in the lower reaches of the Surabaya River (Indonesia) are presented in (Lestari et al. 2020). This river is a source of raw water, used for irrigation, for dumping household and industrial waste. More than 43 MP particles per cubic meter were in the surface level of the river. The MP content reached 34.6 units per m3 in the bottom layer. The MP content at medium depths was noticeably lower (0.76–12.6 units/m^3). Large MP films of 1–5 mm in size made of polyethylene and polypropylene prevailed at all depths.

These experimental studies show that MP particles of small size or density, as well as in the form of fibers or films, are concentrated near the surface of watercourses. MP particles of higher density and regular shape (beads, short cylinders) are located in the bottom layer of the river or are deposited on the bottom. The distribution of MP over the depth of the watercourse depends on the hydraulic particle size and characteristics of the river. The hydraulic particle size W_S is the rate of its steady-state deposition in still water.

The purpose of this work is to develop a method for constructing the distribution of MP in depth depending on the size, density, shape of particles and average flow velocity. MP fibers have their own characteristics (Naumov 2020a) and are not considered here.

4.2 Materials and Methods

4.2.1 Velocity of Particles MP Steady Deposition

The importance of correctly determining the WS value for the particle depth distribution is indicated in a number of papers (Dietrich 1982; Haider and Levenspiel 1989; Khatmullina and Isachenko 2017; Shraiber et al. 1990; Velikanov and Naumov 2014; Zhiyao et al. 2008). There are two main approaches.

The first approach is to use experimental data to obtain regression dependences of the deposition rate on the determining parameters. Dietrich (1982) used the dimensionless velocity W_*, the diameter D_*, and the Corey shape coefficient *csf*:

$$W_* = \frac{W_s^3}{G\nu},\ D_* = \frac{D_n^3 G}{\nu^2},\ G = g\frac{\rho_s - \rho_f}{\rho_f},\ csf = \frac{c}{(a \cdot b)^{0.5}} \tag{4.1}$$

where D_n is nominal (also called equivalent) particle diameter equal to the diameter of a sphere of the same volume as the particle; ν is the kinematic viscosity coefficient of the liquid; g is the acceleration of free fall; ρ_f, ρ_s are the density of fluid and particles, respectively; *a, b* and *c* are longest, middle and shortest axis of the particle in three orthogonal planes, respectively.

The second approach (Haider and Levenspiel 1989; Shraiber et al. 1990; Velikanov and Naumov 2014) is based on the fundamental laws of hydromechanics. The standard resistance curve of a sphere in a viscous medium is used in the second approach. The geometric shape coefficient is used to account for the shape of particles (Shraiber et al. 1990):

$$\xi\ =\ S/S_0,\ S_0\ =\ (36\pi V^2)^{1/3} \tag{4.2}$$

where *S, V* are the surface area and volume of an arbitrary particle; S_0 is the surface area of a spherical particle of equal volume.

The sphericity coefficient $\phi = 1/\xi$ (Haider and Levenspiel 1989) is usually used in English-language publications.

The influence of differences in the particle shape from spherical coefficient of hydrodynamic resistance in the second approach takes into account the dynamic shape factor Γ.

Typically, the following formula is used:

$$C_\Gamma\ =\ \Gamma \cdot C_R(Re),\ =\ D_n \cdot W\nu \tag{4.3}$$

where C_R is the coefficient of hydrodynamic drag of a sphere in a boundless viscous medium; *Re* is the Reynolds number; *W* is the velocity of the particle relative to the liquid.

The coefficient Γ is a function of ξ and Re in the general case. The correction depends only on the geometric shape coefficient in the linear ($Re < 1$) and quadratic drag ($Re > 1000$) (Velikanov and Naumov 2014):

$$\Gamma_1(\xi) = 1 + 0.348 \cdot (\xi - 1),\ \Gamma_2(\xi) = 10.0 - 9.0/\xi \tag{4.4}$$

The transition drag region is the least explored. Moreover, the most deposition of MP occurs in this area. In our opinion, it is advisable to use the formula obtained in (Kondratev et al. 2016) from (4.4) in the transition drag region:

$$C_\Gamma = \left(\frac{24}{\mathrm{Re}} + \frac{53}{32 + \mathrm{Re}}\right) \cdot \Gamma_1(\xi) + 0.44 \cdot \Gamma_2(\xi) \tag{4.5}$$

Formula (4.5) is quite simple. The results of the calculation are consistent with the experimental data, at least as well as with the formulas of other authors.

The steady-state settling velocity of a dispersed particle can be found from a nonlinear equation. This equation does not have an analytical solution in the general case:

$$3\gamma \cdot D_n \cdot C_\Gamma\left(\frac{D_n W_s}{\nu}, \xi\right) \cdot W_s^2 = 4g(1-\gamma),\ \gamma = \frac{\rho_f}{\rho_s} \tag{4.6}$$

Using the numerical method to find the WS from (4.6) could have caused difficulties 50 years ago. This problem is easily solved at present, for example, in the Mathcad (Naumov 2020b).

4.2.2 The Distribution of Particles MP Over the Watercourse Depth

The distribution of MP over depth depends on the action of gravity on suspended particles and the effect of turbulent water velocity pulsations. The long straight channel with a constant depth H and an average water velocity U_S is further considered. Large inertial particles are absent in this flow in the suspended state. They've all fallen to the bottom. The remaining small low-inertia particles form a background turbidity. They are in dynamic equilibrium. As many particles settle on the bottom, the same amount rises from the bottom. The average local turbidity of the watercourse does not change.

We assume that the MP impurity can be considered passive, and the velocity profiles of the carrier medium (water) are known. The distribution of each impurity fraction can be considered independently of the others. The vertical coordinate Z is counted from the bottom.

The change in the content of suspended MP particles over the flow depth is described by the turbulent diffusion equation. The diffusion equation can be simplified in a steady flow without particle deposition (Velikanov and Naumov 2014; Velikanov and Naumov 2017):

$$\frac{\partial}{\partial Z}\left(D_z \frac{\partial B_i}{\partial Z}\right) + W_i \frac{\partial B_i}{\partial Z} = 0 \tag{4.7}$$

where D_z is the coefficient of vertical turbulent diffusion; B_i is the concentration of the i-th fraction of MP; W_i is the settling rate of the i-th fraction (hydraulic fineness).

We can write for a power model of the longitudinal velocity profile of a watercourse U (Volynov 2013):

$$U = U_{max} \cdot z^{nu},\ z = \frac{Z}{H},\ \frac{U_{max}}{U_s} = nu + 1,\ nu = \frac{\sqrt{g}}{0.4Cs} \tag{4.8}$$

where nu is the exponent in the vertical velocity profile; Cs is the Chezy coefficient.

The vertical turbulent diffusion coefficient, which varies in depth, is calculated using the formula from (Volynov 2013):

$$D_z = \frac{g \cdot H \cdot U_s(1-z)}{(1+nu) \cdot Cs^2 \cdot nu \cdot z^{nu-1}} \tag{4.9}$$

The formula for the profile of the dimensionless impurity concentration MP is obtained by substituting (4.9) in (4.7) and integrating:

$$b_i(z) = \frac{B_i(z)}{B_i(0)} = exp\left(-\frac{(nu+1) \cdot W_{si}}{0.16 \cdot nu \cdot U_s} \cdot \int_0^z \frac{d\eta}{\eta^{1-nu}(1-\eta)}\right) \tag{4.10}$$

where $B_i(0)$ is the concentration of the i-th MP fraction at the bottom.

4.3 Results

We calculate the steady-state settling velocity under experimental conditions (Khatmullina and Isachenko 2017) using formulas (4.4)–(4.6). Polycaprolactone (PCL) density $\rho S = 1131$ kg/m^3; cylinder diameter range D = 0.59–5.09 mm; cylinder elongation $\lambda \equiv$ L/D = 0.6–1.26; kinematic water viscosity coefficient $\nu = 0.872 \cdot 10$–6 m^2/s. Let's express the geometric shape coefficient and the equivalent cylinder diameter in terms of elongation:

$$\xi = \frac{\lambda + 0.5}{(1.5 \cdot \lambda)^{2/3}}, \; D_n = D \cdot (1.5 \cdot \lambda)^{1/3} \tag{4.11}$$

The results of calculating the settling velocity of cylinders with two elongation values of 0.6 and 1.26 are shown in Fig. 4.1.

The results of calculating the MP distribution over the watercourse depth using the formula (4.10) are shown in Figs. 4.2, 4.3, 4.4, 4.5. In all cases, $b_i(0) = 1$ (the lower right point of the graphs).

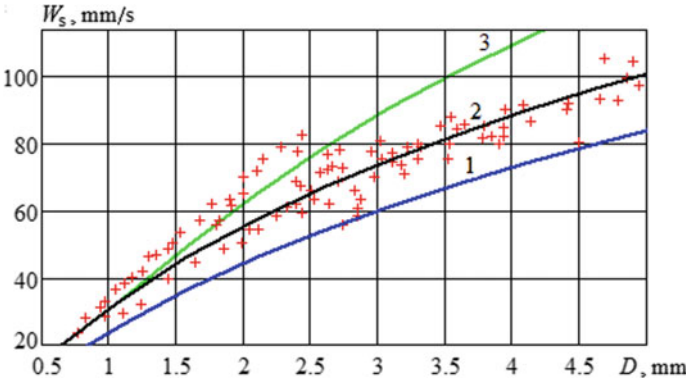

Fig. 4.1 Dependence of the settling velocity of the PCL cylinders on the diameter. Points are experimental data (Khatmullina and Isachenko 2017). Curves are calculation results for (3)–(5): 1—cylinders at $\lambda = 0.6$; 2—cylinders at $\lambda = 1.26$; 3—deal spheres (compiled by the authors)

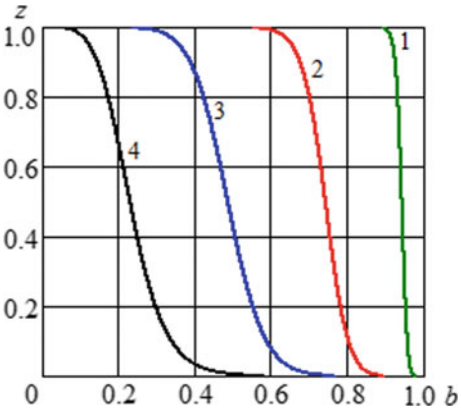

Fig. 4.2 Effect of the MP size on the distribution ($\rho_S =$ 1131 kg/m^3; $\xi = 1.6$; $U_S. =$ 0.15 m/s): 1 – $D_n =$ 0.02 mm; 2 – $D_n =$ 0.045 mm; 3 – $D_n =$ 0.070 mm; 4 – $D_n =$ 0.10 mm (compiled by the authors)

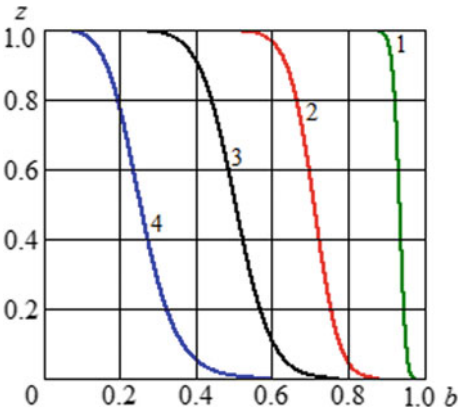

Fig. 4.3 Effect of MP density on the distribution ($D_n = 0.045$ mm; $\xi = 1.6$; $U_S. = 0.15$ m/s): 1 – $\rho_S =$ 1030 kg/m^3; 2 – $\rho_S =$ 1150 kg/m^3; 3 – $\rho_S =$ 1300 kg/m^3; 4 – $\rho_S =$ 1600 kg/m^3 (compiled by the authors)

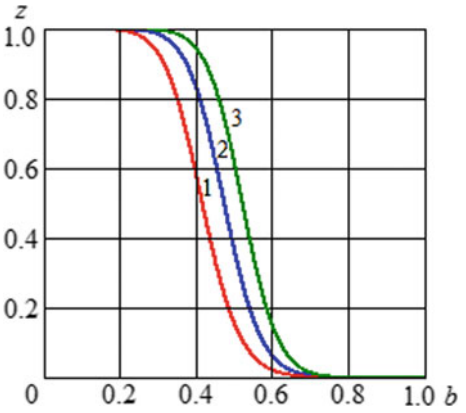

Fig. 4.4 Effect of the MP shape coefficient on the distribution ($D_n = 0.07$ mm; $\rho_S = 1131$ kg/m^3; $U_S. =$ 0.15 m/s): 1 – $\xi = 1.0$; 2 – ξ = 1.5; 3 – $\xi = 2.0$ (compiled by the authors)

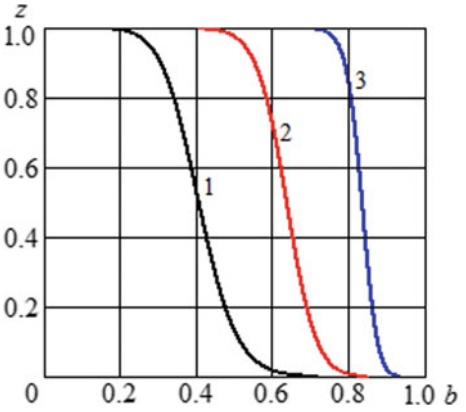

Fig. 4.5 Effect of water flow velocity on the distribution ($D_n = 0.045$ mm; $\rho_S =$ 1131 kg/m^3; $\xi = 1.6$): 1 – $U_S. = 0.05$ m/s; 2 – $U_S.$ = 0.1 m/s; 3 – $U_S. = 0.3$ m/s (compiled by the authors)

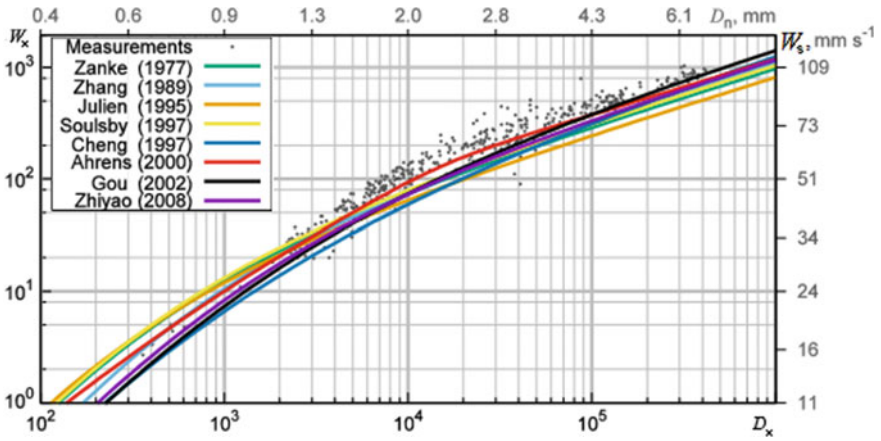

Fig. 4.6 Dimensionless settling velocity of polycaprolactone cylinders (points are experimental data) and calculated curves. Figure taken from (Khatmullina and Isachenko 2017)

4.4 Discussion

Quite complex regression dependences of W* on D* and csf were obtained in (Dietrich 1982). Obtaining new experimental data in the first approach requires selecting new empirical coefficients in a known relationship or proposing a new regression function. This approach is not fundamental and does not allow us to identify errors and experimental errors. A significant part of the experimental data in Fig. 4.6 from (Khatmullina and Isachenko 2017) is located above the calculated curves of various authors from the review (Zhiyao et al. 2008).

All the samples in the experiments (Khatmullina and Isachenko 2017) had elongation values of 0.6 and 1.26. Therefore, the experimental points in Fig. 4.1 should lie between curves 1 and 2. But many of them lie above curve 2. Moreover, some of the points lie even above curve 3, which is constructed for ideal spheres. The result was an overestimation of the settling velocity of cylindrical MP particles in (Khatmullina and Isachenko 2017). Most likely, there was a systematic error.

4.5 Conclusion

For MP particles with a density of 1131 kg/m^3 and an equivalent diameter of less than 20 microns, the vertical distribution in the watercourse differs little from uniform. With increasing D_n, the unevenness of the profile increases. The results of the study showed that a significant part of the MP with a high density moves near the bottom, even if the particles are small in size, and a decrease in the velocity of the watercourse leads to an increase in the uneven distribution of MP on the vertical. The geometric

coefficient of the particle shape with a change from 1 to 2 slightly affects the distribution of MP in depth. As a rule, when assessing the contamination of a water body with microplastics, they are limited to sampling from the surface layer, which does not provide complete information about its condition. The method proposed by the authors for constructing the distribution of MP by depth, depending on the shape, size and density of particles, as well as the average flow velocity, will allow us to estimate the average concentration of MP measured in the surface layer over the entire depth of the flow (vertically). This method can be used when conducting environmental studies on watercourses.

References

Andrady AL (2011) Microplastics in the marine environment. Mar Pollut Bull 62:1596–1605
Castañeda RA, Avlijas S, Simard MA, Ricciardi A (2014) Microplastic pollution in St. Lawrence river sediments. Canadian J. Fisheries and Aquatic Sciences 71:1767–1771
Chubarenko I, Stepanova N (2017) Microplastics in sea coastal zone: lessons learned from the Baltic amber. Environ Pollut 224:243–254. https://doi.org/10.1016/j.envpol.2017.01.085
Cózar A, Echevarría F, González-Gordillo JI, Irigoien X, Ubeda B, Hernández-León S, Palma AT, Duarte CM (2014) Plastic debris in the open ocean. Proc Natl Acad Sci 111(28):10239–10244
Dietrich WE (1982) Settling velocity of natural particles. Water Resour Res 18:1615–1626
Erni-Cassola G, Zadjelovic V, Matthew I, Gibson MI, Christie-Oleza JA (2019) Distribution of plastic polymer types in the marine environment. J. Hazardous Materials 369:691–698
Haider A, Levenspiel O (1989) Drag coefficient and therminal velocity of spherical and nonspherical particles. Powder Technol 58:63–70
Han M, Niu X, Tang M, Zhang B, Wang G, Yue W, Kong W, Zhu J (2020) Distribution of microplastics in surface water of the lower Yellow River near estuary. Sci Total Environ 707:135601
Khatmullina L, Isachenko I (2017) Settling velocity of microplastic particles of regular shapes. Mar Pollut Bull 114:871–880
Kondratev AS, Nya TL, Shvydko PP (2016) Calculation of hydraulic drag coefficient of arbitrary shape solid particles. Fundamental Research 11:286–292
Lestari P, Trihadiningrum Y, Wijaya BA, Yunus KA, Firdaus M (2020) Distribution of microplastics in Surabaya River. Indonesia. Science Total Environment 726:138560
Mani T, Hauk A, Walter U, Burkhardt-Holm P (2015) Microplastics profile along the Rhine River. Sci Rep 5:179–188
Naumov VA (2020a) Law of distribution of breaking elongation of yarn. Fibre Chem 51:244–246
Naumov, V. A. (2020b). Influence of leakage on characteristics of the vacuum transport unit based on the water-ring pump. IOP Conf. Series: Materials Science and Engineering, 862, 032007.
Moore CJ, Lattin GL, Zellers AF (2011) Quantity and type of plastic debris flowing from two urban rivers to coastal waters and beaches of Southern California. J. Integrated Coastal Management 11:65–73
Shraiber AA, Gavin LB, Naumov VA, Yatsenko VP (1990) Turbulent Flows in Gas Suspensions. Hemisphere, New York, p 248
Velikanov NL, Naumov VA (2014) Suspended particles in a water stream and their deposition. Water: chemistry and ecology, 2, 114–119. (In Russian)
Velikanov NL, Naumov VA (2017) Modeling of the distribution of suspended organic impurities in watercourses. Water: chemistry and ecology, 3, 3–8 (In Russian)
Volynov MA (2013) Influence of the planned geometry of the riverbed on the diffusion and dispersion of impurity. Fundamental Research 6:535–540

Zhang L, Liu J, Xie Y, Zhong S, Yang B, Lu D, Zhong Q (2020) Distribution of microplastics in surface water and sediments of Qin river in Beibu Gulf, China. Sci Total Environ 708:135–176
Zhiyao S, Tingting W, Fumin X, Ruijie L (2008) A simple formula for predicting settling velocity of sediment particles. Water Science and Engineering 1:37–43